11

Mathematical Modelling of Dynamics of Boiler Surfaces Heated Convectively

Wiesław Zima
Cracow University of Technology
Poland

1. Introduction

In order to increase the efficiency of electrical power production, steam parameters, namely pressure and temperature, are increased. Changes in the superheated steam and feed water temperatures in boiler operation are also caused by changes in the heat transfer conditions on the combustion gases side. When the waterwalls of the furnace chamber undergo slagging up, the combustion gases temperature at the furnace chamber outlet increases, and the superheaters and economizers take more heat. In order to maintain the same temperature of the superheated steam at the outlet, the flow of injected water must be increased. Upon cleaning the superheater using ash blowers, the heat flux taken by the superheater also increases, which in turn changes the coolant mass flow. Changes of the superheated steam and feed water temperatures caused by switching off some burners or coal pulverizers or by varying the net calorific value of the supplied coal may also be significant. Precise modelling of superheater dynamics to improve the quality of control of the superheated steam temperature is therefore essential. Designing the mathematical model describing superheater dynamics is also very important from the point of view of digital control of the superheated steam temperature. A crucial condition for its proper control is setting up a precise numerical model of the superheater which, based on the measured inlet and outlet steam temperature at the given stage, would provide fast and accurate determination of the water mass flow to the injection attemperator. Such a mathematical model fulfils the role of a process "observer", significantly improving the quality of process control (Zima, 2003, 2006). The transient processes of heat and flow occurring in superheaters and economizers are complex and highly nonlinear. That complexity is caused by the high values of temperature and pressure, the cross-parallel or cross-counter-flow of the fluids, the large heat transfer surfaces (ranging from several hundred to several thousand square metres), the necessity of taking into account the increasing fouling of these surfaces on the combustion gases side, and the resulting change in heat transfer conditions. The task is even more difficult when several heated surfaces are located in parallel in one combustion gas duct, an arrangement which is applied quite often. Nonlinearity results mainly from the dependency of the thermo-physical properties of the working fluids and the separating walls on the pressure and temperature or on the temperature only. Assumption of constancy of these properties reduces the problem to steady state analysis. Diagnosis of heat flow processes in power engineering is generally

based on stabilized temperature conditions. This is due to the absence of mathematical models that apply to big power units under transient thermal conditions (Krzyżanowski & Głuch, 2004). The existing attempts to model steam superheaters and economizers are based on greatly simplified one-dimensional models or models with lumped parameters (Chakraborty & Chakraborty, 2002; Enns, 1962; Lu, 1999; Mohan et al., 2003). Shirakawa presents a dynamic simulation tool that facilitates plant and control system design of thermal power plants (Shirakawa, 2006). Object-oriented modelling techniques are used to model individual plant components. Power plant components can also be modelled using a modified neural network structure (Mohammadzaheri et al., 2009). In the paper by Bojić and Dragićević a linear programming model has been developed to optimize the performance and to find the optimal size of heating surfaces of a steam boiler (Bojić & Dragićević, 2006). In this chapter a new mathematical method for modelling transient processes in convectively heated surfaces of boilers is proposed. It considers the superheater or economizer model as one with distributed parameters. The method makes it possible to model transient heat transfer processes even in the case of fluids differing considerably in their thermal inertias.

2. Description of the proposed model

Real superheaters and economizers are three-dimensional objects. The basic assumptions of the proposed model refer to the parameters of the working fluids. It was assumed that there are no changes in combustion gases flow and temperature in the arbitrary cross-section of the given superheater or economizer stage (Dechamps, 1995). The same applies to steam and feed water. When the real heat exchanger is operating in cross-counter-flow or cross-parallel-flow and has more than four tube rows, its one-dimensional model (double pipe heat exchanger), represented by Fig. 1, can be based on counter-flow or parallel-flow only (Hausen, 1976). In the proposed model, which has distributed parameters, the computations are carried out in the direction of the heated fluid flow in one tube. The tube is equal in size to those installed in the existing object and is placed, in the calculation model, centrally in a larger externally insulated tube of assumed zero wall thickness (Fig. 1). The cross-section A_{cg} of the combustion gases flow results, in the computation model, from dividing the total free cross-section of combustion gases flow by the number of tubes. The mass flows of the working fluids are also related to a single tube.

A precise mathematical model of a superheater, based on solving equations describing the laws of mass, momentum, and energy conservation, is presented in (Zima, 2001, 2003, 2004, 2006). The model makes it possible to determine the spatio-temporal distributions of the mass flow, pressure, and enthalpy of steam in the on-line mode. This chapter presents a model based solely on the energy equation, omitting the mass and momentum conservation equations. Such a model results in fewer final equations and a simpler form. Their solution is thereby reached faster. The short time taken by the computations (within a few seconds) is very important from the perspective of digital temperature control of superheated steam. In the papers by Zima that control method was presented for the first time (Zima, 2003, 2004, 2006). In this case the mathematical model fulfils the role of a process "observer", significantly improving the quality of process control. The omission of the mass and momentum balance equations does not generate errors in the computations and does not constitute a limitation of the method. The history of superheated steam mass flow is not a

rapidly changing one. Also taking into consideration the low density of the steam, it is possible to neglect the variation of steam mass existing in the superheater. Feed water mass flow also does not change rapidly. Moreover the water is an incompressible medium. The results of the proposed method are very similar to results obtained using equations describing the laws of mass, momentum, and energy conservation (Zima, 2001, 2004).
The suggested in this chapter 1D model is proposed for modelling the operation of superheaters and economizers considering time-dependent boundary conditions. It is based on the implicit finite-difference method in an iterative scheme (Zima, 2007).

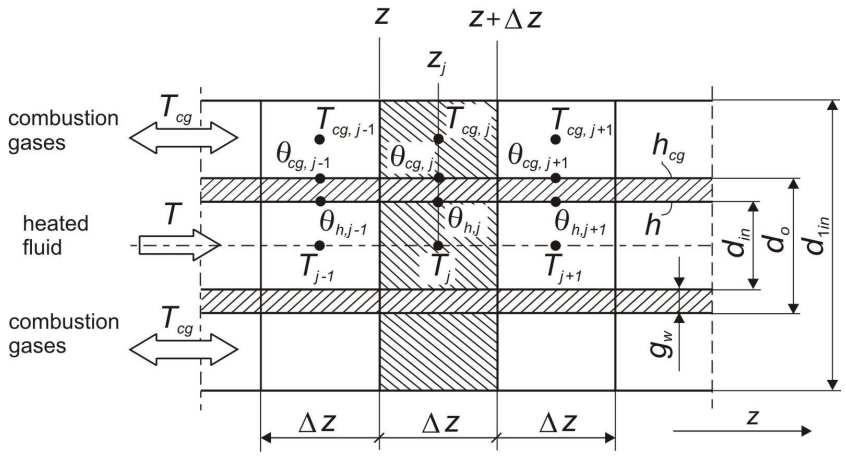

Fig. 1. Analysed control volume of double-pipe heat exchanger

Every equation presented in this section is based on the geometry shown in Fig. 1 and refers to one tube of the heated fluid. The Cartesian coordinate system is used.
The proposed model shows the same transient behaviour as the existing superheater or economizer if:

a. the steam or feed water tube has the same inside and outside diameter, the same length, and the same mass as the real one
b. all the thermo-physical properties of the fluids and the material of the separating walls are computed in real time
c. the time-spatial distributions of heat transfer coefficients are computed in the on-line mode, considering the actual tube pitches and cross-flow of the combustion gases
d. the appropriate free cross-sectional area for the combustion gases flow is assumed in the model:

$$A_{cg} = \frac{A_{cg,t}}{n} = \frac{\pi\left(d_{1in}^2 - d_o^2\right)}{4} \tag{1}$$

e. mass flow of the heated fluid is given by:

$$\dot{m} = \frac{\dot{m}_t}{n} \tag{2}$$

f. mass flow of the combustion gases is given by:

$$\dot{m}_{cg} = \frac{\dot{m}_{cg,t}}{n}. \tag{3}$$

In the above equations:

$A_{cg,t}$ – total free cross-section of combustion gases flow, m²,
$\dot{m}_{cg,t}$ – total combustion gases mass flow, kg/s,
$\dot{m}_t$ – total heated fluid mass flow, kg/s,
n – number of tubes.

The temperature θ of the separating wall is determined from the equation of transient heat conduction:

$$c_w(\theta)\rho_w(\theta)\frac{\partial\theta}{\partial t} = \frac{1}{r}\frac{\partial}{\partial r}\left[rk_w(\theta)\frac{\partial\theta}{\partial r}\right], \tag{4}$$

where:

c_w – specific heat of the tube wall material, J/(kg K),
k_w – thermal conductivity of the tube wall material, W/(mK),
ρ_w – density of the tube wall material, kg/m³.

In order to obtain greater accuracy of the results, the wall is divided into two control volumes. This division makes it possible to determine the temperature on both surfaces of the separating wall, namely θ_{cg} at the combustion gases side and θ_h at the heated medium side (Fig. 2).

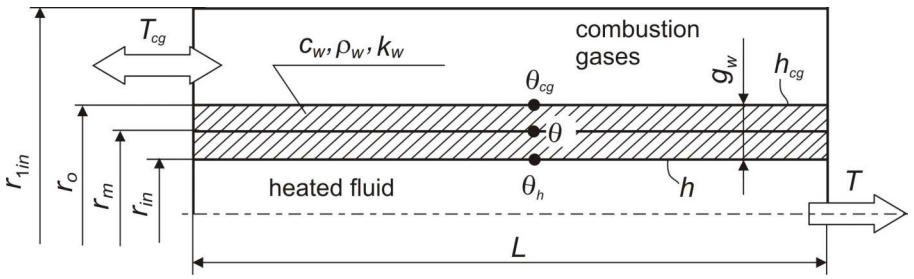

Fig. 2. Tube wall divided into two control volumes

After some transformations, the following formulae are obtained from Equation 4:

$$c_w(\theta_h)\rho_w(\theta_h)\frac{\left(r_m^2 - r_{in}^2\right)}{2}\frac{\partial\theta_h}{\partial t} = \left[rk_w(\theta)\frac{\partial\theta}{\partial r}\right]_{r=r_m} - \left[rk_w(\theta)\frac{\partial\theta}{\partial r}\right]_{r=r_{in}}, \tag{5}$$

$$c_w(\theta_{cg})\rho_w(\theta_{cg})\frac{\left(r_o^2 - r_m^2\right)}{2}\frac{\partial\theta_{cg}}{\partial t} = \left[rk_w(\theta)\frac{\partial\theta}{\partial r}\right]_{r=r_o} - \left[rk_w(\theta)\frac{\partial\theta}{\partial r}\right]_{r=r_m}. \tag{6}$$

Taking into consideration the boundary conditions:

$$k_w(\theta)\frac{\partial\theta}{\partial r}\bigg|_{r=r_{in}} = h\left(\theta\big|_{r=r_{in}} - T\right) = h(\theta_h - T), \tag{7}$$

$$k_w(\theta)\frac{\partial\theta}{\partial r}\bigg|_{r=r_m} = k_w(\theta_m)\frac{\theta_{cg} - \theta_h}{r_o - r_{in}}, \tag{8}$$

$$k_w(\theta)\frac{\partial\theta}{\partial r}\bigg|_{r=r_o} = h_{cg}\left(T_{cg} - \theta\big|_{r=r_o}\right) = h_{cg}\left(T_{cg} - \theta_{cg}\right), \tag{9}$$

where:
h and h_{cg} – heat transfer coefficients at the sides of heated fluid and combustion gases, respectively, W/(m²K),
the following ordinary differential equations are obtained:

$$\frac{\mathrm{d}\theta_h}{\mathrm{d}t} = B\left(\theta_{cg} - \theta_h\right) + C\left(T - \theta_h\right), \tag{10}$$

$$\frac{\mathrm{d}\theta_{cg}}{\mathrm{d}t} = D\left(T_{cg} - \theta_{cg}\right) + E\left(\theta_h - \theta_{cg}\right). \tag{11}$$

In the above equations:

$$B = \frac{\pi d_m k_w(\theta_m)}{A_h c_w(\theta_h)\rho_w(\theta_h) g_w},\quad d_m = \frac{d_{in} + d_o}{2},\quad \theta_m = \frac{\theta_{cg} + \theta_h}{2},\quad C = \frac{h\pi d_{in}}{A_h c_w(\theta_h)\rho_w(\theta_h)},$$

$$D = \frac{h_{cg}\pi d_o}{A_{cg} c_w\left(\theta_{cg}\right)\rho_w\left(\theta_{cg}\right)},\ E = \frac{\pi d_m k_w(\theta_m)}{A_{cg} c_w\left(\theta_{cg}\right)\rho_w\left(\theta_{cg}\right) g_w},\ A_h = \frac{\pi\left(d_m^2 - d_{in}^2\right)}{4},\ \text{and}\ A_{cg} = \frac{\pi\left(d_o^2 - d_m^2\right)}{4}.$$

The transient temperatures of the combustion gases and heated fluid are evaluated iteratively, using relations derived from the equations of energy balance. In these equations, the change in time of the total energy in the control volume, the flux of energy entering and exiting the control volume, and the heat flux transferred to it through its surface are taken into consideration.
The energy balance equations take the following forms (Fig. 1):

- combustion gases

$$\Delta z A_{cg} c_{cg}\left(T_{cg}\right)\rho_{cg}\left(T_{cg}\right)\frac{\Delta T_{cg}}{\Delta t} = \pm\left(\dot{m}_{cg} i_{cg}\Big|_{z+\Delta z} - \dot{m}_{cg} i_{cg}\Big|_{z}\right) + h_{cg}\pi d_o \Delta z\left(\theta_{cg} - T_{cg}\right), \tag{12}$$

- feed water or steam

$$\Delta z A c(T,p)\rho(T,p)\frac{\Delta T}{\Delta t} = \dot{m}\, i\Big|_{z} - \dot{m}\, i\Big|_{z+\Delta z} + h\pi d_{in}\Delta z\left(\theta_h - T\right), \tag{13}$$

where:
i – specific enthalpy, J/kg,

p – pressure, Pa,

$$A_{cg} = \frac{\pi d_{1in}^2 - \pi d_o^2}{4}, \text{ and } A = \frac{\pi d_{in}^2}{4}.$$

After rearranging and assuming that $\Delta t \to 0$ and $\Delta z \to 0$, the following equations are obtained from (12) and (13), respectively:

$$\frac{\partial T_{cg}}{\partial t} = \pm F \frac{\partial T_{cg}}{\partial z} + G\left(\theta_{cg} - T_{cg}\right), \tag{14}$$

$$\frac{\partial T}{\partial t} = -H \frac{\partial T}{\partial z} + J\left(\theta_h - T\right). \tag{15}$$

In the above equations:

$$F = \frac{\dot{m}_{cg}}{A_{cg}\rho_{cg}\left(T_{cg}\right)}, \quad G = \frac{h_{cg}\pi d_o}{A_{cg}c_{cg}\left(T_{cg}\right)\rho_{cg}\left(T_{cg}\right)}, \quad H = \frac{\dot{m}}{A\rho\left(T,p\right)} \text{ and } J = \frac{h\pi d_{in}}{Ac\left(T,p\right)\rho\left(T,p\right)}.$$

The sign "+" in Equations (12) and (14) refers to counter-flow, and the sign " – " to parallel-flow. The implicit finite-difference method is proposed to solve the system of Equations (10) to (11) and (14) to (15). The time derivatives are replaced by a forward difference scheme, whereas the dimensional derivatives are replaced by the backward difference scheme in the case of parallel-flow and the forward difference scheme in the case of counter-flow.
After some transformations the following formulae are obtained:

$$\theta_{h,j}^{t+\Delta t} = \frac{1}{K\Delta t}\theta_{h,j}^{t} + \frac{C}{K}T_j^{t+\Delta t} + \frac{B}{K}\theta_{cg,j}^{t+\Delta t}, \qquad j = 1, ..., M; \tag{16}$$

$$\theta_{cg,j}^{t+\Delta t} = \frac{1}{L\Delta t}\theta_{cg,j}^{t} + \frac{D}{L}T_{cg,j}^{t+\Delta t} + \frac{E}{L}\theta_{h,j}^{t+\Delta t}, \qquad j = 1, ..., M; \tag{17}$$

$$T_{cg,j}^{t+\Delta t} = \frac{1}{P\Delta t}T_{cg,j}^{t} + \frac{F}{P\Delta z}T_{cg,j\pm1}^{t+\Delta t} + \frac{G}{P}\theta_{cg,j}^{t+\Delta t}, \tag{18}$$

$$T_j^{t+\Delta t} = \frac{1}{Q\Delta t}T_j^{t} + \frac{H}{Q\Delta z}T_{j-1}^{t+\Delta t} + \frac{J}{Q}\theta_{h,j}^{t+\Delta t}, \qquad j = 2, ..., M; \tag{19}$$

where:
M – number of cross-sections,

$$K = \frac{1}{\Delta t} + B + C, \quad L = \frac{1}{\Delta t} + D + E, \quad P = \frac{1}{\Delta t} + \frac{F}{\Delta z} + G, \text{ and } Q = \frac{1}{\Delta t} + \frac{H}{\Delta z} + J.$$

In Equation (18), $j = 2, \ldots, M$ for parallel-flow (sign "−") and $j = 1, \ldots, M-1$ for counter-flow (sign "+").
Considering the small temperature drop on the thickness of the wall (≈ 3–4 K), Equation (4) can also be solved assuming only one control volume. The result will be a formula determining only the mean temperature θ of a wall (Fig. 2).

In this case, after some transformations, Equation (4) takes the following form:

$$c_w(\theta)\rho_w(\theta)\frac{\left(r_o^2-r_{in}^2\right)}{2}\frac{\partial\theta}{\partial t}=\left[rk_w(\theta)\frac{\partial\theta}{\partial r}\right]\Bigg|_{r=r_o}-\left[rk_w(\theta)\frac{\partial\theta}{\partial r}\right]\Bigg|_{r=r_{in}}. \tag{20}$$

Taking into consideration the boundary conditions described by Equations (7) and (9), the following ordinary differential equation is obtained:

$$\frac{\mathrm{d}\theta}{\mathrm{d}t}=U\left(T_{cg}-\theta\right)+V\left(T-\theta\right). \tag{21}$$

Replacing the time derivative by the forward difference scheme, after rearranging we obtain:

$$\theta_j^{t+\Delta t}=\frac{1}{W\Delta t}\theta_j^t+\frac{U}{W}T_{cg,j}^{t+\Delta t}+\frac{V}{W}T_j^{t+\Delta t}, \tag{22}$$

where:

$$U=\frac{h_{cg}d_o}{c_w(\theta)\rho_w(\theta)g_w d_m},\quad V=\frac{hd_{in}}{c_w(\theta)\rho_w(\theta)g_w d_m},\quad d_m=\frac{d_o+d_{in}}{2}\ \text{and}\ W=\frac{1}{\Delta t}+U+V.$$

The suggested method is also suitable for modelling the dynamics of several surfaces heated convectively, often placed in parallel in a single gas pass of the boiler.
As an example of these surfaces it was assumed that the feed water heater and superheater are located in parallel in such a gas pass (Fig. 3). Additionally, the flow of combustion gases is in parallel-flow with feed water and simultaneously in counter-flow to steam.
The equation of transient heat conduction (Equation 4) takes the following forms (the walls of steam and feed water pipes are divided into two control volumes):

- wall of steam pipe

$$c_w(\theta_{1s})\rho_w(\theta_{1s})\frac{\left(r_m^2-r_{in}^2\right)}{2}\frac{\partial\theta_{1s}}{\partial t}=\left[rk_w(\theta_1)\frac{\partial\theta_1}{\partial r}\right]\Bigg|_{r=r_m}-\left[rk_w(\theta_1)\frac{\partial\theta_1}{\partial r}\right]\Bigg|_{r=r_{in}}, \tag{23}$$

$$c_w\left(\theta_{1cg}\right)\rho_w\left(\theta_{1cg}\right)\frac{\left(r_o^2-r_m^2\right)}{2}\frac{\partial\theta_{1cg}}{\partial t}=\left[rk_w(\theta_1)\frac{\partial\theta_1}{\partial r}\right]\Bigg|_{r=r_o}-\left[rk_w(\theta_1)\frac{\partial\theta_1}{\partial r}\right]\Bigg|_{r=r_m}, \tag{24}$$

- wall of economizer pipe

$$c_w\left(\theta_{2fw}\right)\rho_w\left(\theta_{2fw}\right)\frac{\left(r_{2m}^2-r_{2in}^2\right)}{2}\frac{\partial\theta_{2fw}}{\partial t}=\left[rk_w(\theta_2)\frac{\partial\theta_2}{\partial r}\right]\Bigg|_{r=r_{2m}}-\left[rk_w(\theta_2)\frac{\partial\theta_2}{\partial r}\right]\Bigg|_{r=r_{2in}}, \tag{25}$$

$$c_w\left(\theta_{2cg}\right)\rho_w\left(\theta_{2cg}\right)\frac{\left(r_{2o}^2-r_{2m}^2\right)}{2}\frac{\partial\theta_{2cg}}{\partial t}=\left[rk_w(\theta_2)\frac{\partial\theta_2}{\partial r}\right]\Bigg|_{r=r_{2o}}-\left[rk_w(\theta_2)\frac{\partial\theta_2}{\partial r}\right]\Bigg|_{r=r_{2m}}. \tag{26}$$

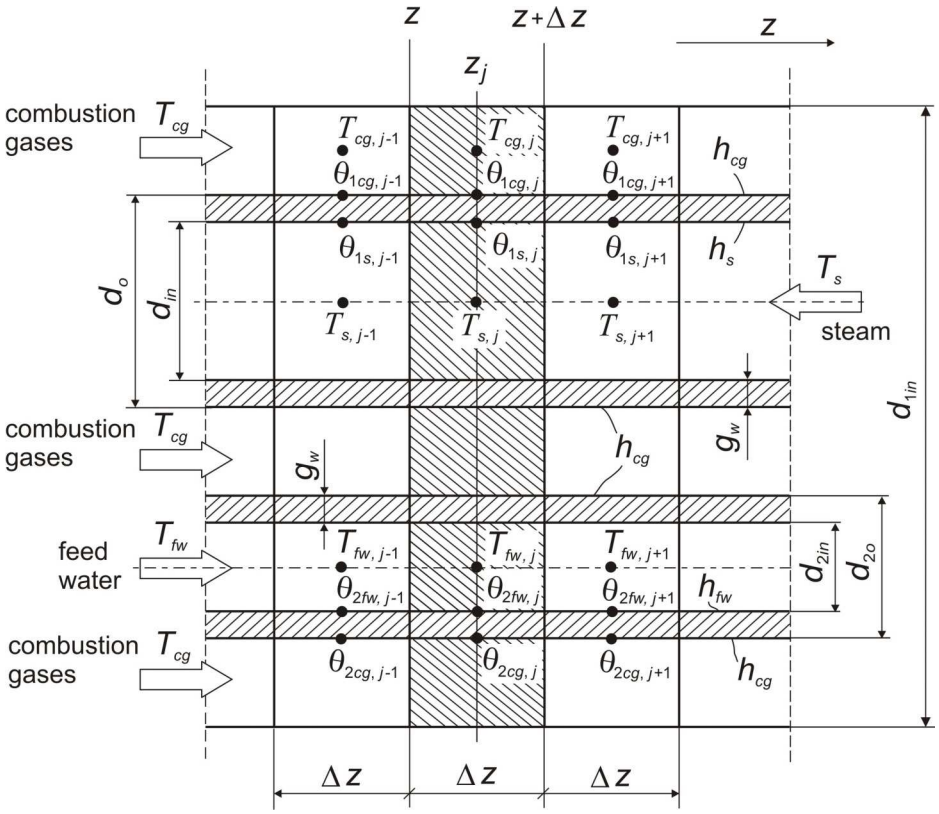

Fig. 3. Analysed control volume of several surfaces heated convectively, placed in parallel in a single gas pass

Substituting the appropriate boundary conditions, the following differential equations are obtained after some transformations:

$$\frac{\mathrm{d}\theta_{1s}}{\mathrm{d}t} = B_1\left(\theta_{1cg} - \theta_{1s}\right) + C_1\left(T_s - \theta_{1s}\right), \tag{27}$$

$$\frac{\mathrm{d}\theta_{1cg}}{\mathrm{d}t} = D_1\left(T_{cg} - \theta_{1cg}\right) + E_1\left(\theta_{1s} - \theta_{1cg}\right), \tag{28}$$

$$\frac{\mathrm{d}\theta_{2fw}}{\mathrm{d}t} = F_1\left(\theta_{2cg} - \theta_{2fw}\right) + G_1\left(T_{fw} - \theta_{2fw}\right), \tag{29}$$

$$\frac{\mathrm{d}\theta_{2cg}}{\mathrm{d}t} = H_1\left(T_{cg} - \theta_{2cg}\right) + J_1\left(\theta_{2fw} - \theta_{2cg}\right). \tag{30}$$

In the above equations:

$$B_1 = \frac{k_w(\theta_{1m})\pi d_m}{A_{1s}c_w(\theta_{1s})\rho_w(\theta_{1s})g_w},\quad C_1 = \frac{h_s\pi d_{in}}{A_{1s}c_w(\theta_{1s})\rho_w(\theta_{1s})},\quad D_1 = \frac{h_{cg}\pi d_o}{A_{1cg}c_w\left(\theta_{1cg}\right)\rho_w\left(\theta_{1cg}\right)},$$

$$E_1 = \frac{k_w(\theta_{1m})\pi d_m}{A_{1cg}c_w\left(\theta_{1cg}\right)\rho_w\left(\theta_{1cg}\right)g_w},\quad F_1 = \frac{k_w(\theta_{2m})\pi d_{2m}}{A_{2fw}c_w\left(\theta_{2fw}\right)\rho_w\left(\theta_{2fw}\right)g_w},\quad G_1 = \frac{h_{fw}\pi d_{2in}}{A_{2fw}c_w\left(\theta_{2fw}\right)\rho_w\left(\theta_{2fw}\right)},$$

$$H_1 = \frac{h_{cg}\pi d_{2o}}{A_{2cg}c_w\left(\theta_{2cg}\right)\rho_w\left(\theta_{2cg}\right)},\quad J_1 = \frac{k_w(\theta_{2m})\pi d_{2m}}{A_{2cg}c_w\left(\theta_{2cg}\right)\rho_w\left(\theta_{2cg}\right)g_w},\quad \theta_{1m} = \frac{\theta_{1s}+\theta_{1cg}}{2},$$

$$\theta_{2m} = \frac{\theta_{2fw}+\theta_{2cg}}{2},\quad d_m\frac{d_{in}+d_o}{2},\quad d_{2m}\frac{d_{2in}+d_{2o}}{2},\quad A_{1s} = \frac{\pi\left(d_m^2-d_{in}^2\right)}{4},\quad A_{1cg} = \frac{\pi\left(d_o^2-d_m^2\right)}{4},$$

$$A_{2fw} = \frac{\pi\left(d_{2m}^2-d_{2in}^2\right)}{4},\ \text{and}\ A_{2cg} = \frac{\pi\left(d_{2o}^2-d_{2m}^2\right)}{4}.$$

The energy balance equations take the following forms (Fig. 3):

- combustion gases

$$\begin{aligned}\Delta z A_{cg}c_{cg}\left(T_{cg}\right)\rho_{cg}\left(T_{cg}\right)\frac{\Delta T_{cg}}{\Delta t} &= \dot{m}_{cg}i_{cg}\Big|_z - \dot{m}_{cg}i_{cg}\Big|_{z+\Delta z}\\ &+h_{cg}\pi d_o\Delta z\left(\theta_{1cg}-T_{cg}\right)+h_{cg}\pi d_{2o}\Delta z\left(\theta_{2cg}-T_{cg}\right)\end{aligned} \tag{31}$$

- steam

$$\Delta z A_s c_s\left(T_s,p_s\right)\rho_s\left(T_s,p_s\right)\frac{\Delta T_s}{\Delta t} = \dot{m}_s i_s\Big|_{z+\Delta z} - \dot{m}_s i_s\Big|_z + h_s\pi d_{in}\Delta z\left(\theta_{1s}-T_s\right), \tag{32}$$

- feed water

$$\Delta z A_{fw}c_{fw}\left(T_{fw},p_{fw}\right)\rho_{fw}\left(T_{fw},p_{fw}\right)\frac{\Delta T_{fw}}{\Delta t} = \dot{m}_{fw}i_{fw}\Big|_z - \dot{m}_{fw}i_{fw}\Big|_{z+\Delta z} + h_{fw}\pi d_{2in}\Delta z\left(\theta_{2fw}-T_{fw}\right), \tag{33}$$

where:

$$A_{cg} = \frac{\pi d_{1in}^2}{4} - \left(\frac{\pi d_o^2}{4}+\frac{\pi d_{2o}^2}{4}\right),\quad A_s = \frac{\pi d_{in}^2}{4},\ \text{and}\ A_{fw} = \frac{\pi d_{2in}^2}{4}.$$

After rearranging and assuming that $\Delta t\to 0$ and $\Delta z\to 0$, the following formulae were obtained (from Equations (31)–(33), respectively):

$$\frac{\partial T_{cg}}{\partial t} = K_1\left(\theta_{1cg}-T_{cg}\right)+L_1\left(\theta_{2cg}-T_{cg}\right)-P_1\frac{\partial T_{cg}}{\partial z}, \tag{34}$$

$$\frac{\partial T_s}{\partial t} = Q_1\left(\theta_{1s} - T_s\right) + R_1 \frac{\partial T_s}{\partial z}, \tag{35}$$

$$\frac{\partial T_{fw}}{\partial t} = S_1\left(\theta_{2\,fw} - T_{fw}\right) - U_1 \frac{\partial T_{fw}}{\partial z}, \tag{36}$$

where:

$$K_1 = \frac{h_{cg}\pi d_o}{A_{cg}c_{cg}\left(T_{cg}\right)\rho_{cg}\left(T_{cg}\right)},\ L_1 = \frac{h_{cg}\pi d_{2o}}{A_{cg}c_{cg}\left(T_{cg}\right)\rho_{cg}\left(T_{cg}\right)},\ P_1 = \frac{\dot{m}_{cg}}{A_{cg}\rho_{cg}\left(T_{cg}\right)},\ R_1 = \frac{\dot{m}_s}{A_s\rho_s\left(T_s, p_s\right)},$$

$$Q_1 = \frac{h_s\pi d_{in}}{A_s c_s\left(T_s, p_s\right)\rho_s\left(T_s, p_s\right)},\ S_1 = \frac{h_{fw}\pi d_{2in}}{A_{fw}c_{fw}\left(T_{fw}, p_{fw}\right)\rho_{fw}\left(T_{fw}, p_{fw}\right)}, \text{ and } U_1 = \frac{\dot{m}_{fw}}{A_{fw}\rho_{fw}\left(T_{fw}, p_{fw}\right)}.$$

To solve the system of Equations (27) to (30) and (34) to (36) the implicit finite-difference method was used. After some transformations the following dependencies were obtained:

$$\theta_{1s,j}^{t+\Delta t} = \frac{1}{V\Delta t}\theta_{1s,j}^{t} + \frac{B_1}{V}\theta_{1cg,j}^{t+\Delta t} + \frac{C_1}{V}T_{s,j}^{t+\Delta t}, \quad j = 1, ..., M; \tag{37}$$

$$\theta_{1cg,j}^{t+\Delta t} = \frac{1}{V_1\Delta t}\theta_{1cg,j}^{t} + \frac{D_1}{V_1}T_{cg,j}^{t+\Delta t} + \frac{E_1}{V_1}\theta_{1s,j}^{t+\Delta t}, \quad j = 1, ..., M; \tag{38}$$

$$\theta_{2\,fw,j}^{t+\Delta t} = \frac{1}{W\Delta t}\theta_{2\,fw,j}^{t} + \frac{F_1}{W}\theta_{2cg,j}^{t+\Delta t} + \frac{G_1}{W}T_{fw,j}^{t+\Delta t}, \quad j = 1, ..., M; \tag{39}$$

$$\theta_{2cg,j}^{t+\Delta t} = \frac{1}{W_1\Delta t}\theta_{2cg,j}^{t} + \frac{H_1}{W_1}T_{cg,j}^{t+\Delta t} + \frac{J_1}{W_1}\theta_{2\,fw,j}^{t+\Delta t}, \quad j = 1, ..., M; \tag{40}$$

$$T_{cg,j}^{t+\Delta t} = \frac{1}{X_1\Delta t}T_{cg,j}^{t} + \frac{K_1}{X_1}\theta_{1cg,j}^{t+\Delta t} + \frac{L_1}{X_1}\theta_{2cg,j}^{t+\Delta t} + \frac{P_1}{X_1\Delta z}T_{cg,j-1}^{t+\Delta t}, \quad j = 2, ..., M; \tag{41}$$

$$T_{s,j}^{t+\Delta t} = \frac{1}{Y_1\Delta t}T_{s,j}^{t} + \frac{Q_1}{Y_1}\theta_{1s,j}^{t+\Delta t} + \frac{R_1}{Y_1\Delta z}T_{s,j+1}^{t+\Delta t}, \quad j = 1, ..., M\text{-}1; \tag{42}$$

$$T_{fw,j}^{t+\Delta t} = \frac{1}{Z_1\Delta t}T_{fw,j}^{t} + \frac{S_1}{Z_1}\theta_{2\,fw,j}^{t+\Delta t} + \frac{U_1}{Z_1\Delta z}T_{fw,j-1}^{t+\Delta t}, \quad j = 2, ..., M. \tag{43}$$

In the above equations:

$$V = \frac{1}{\Delta t} + B_1 + C_1,\quad V_1 = \frac{1}{\Delta t} + D_1 + E_1,\quad W = \frac{1}{\Delta t} + F_1 + G_1,\quad W_1 = \frac{1}{\Delta t} + H_1 + J_1,$$

$$X_1 = \frac{1}{\Delta t} + K_1 + L_1 + \frac{P_1}{\Delta z},\quad Y_1 = \frac{1}{\Delta t} + Q_1 + \frac{R_1}{\Delta z}, \text{ and } \quad Z_1 = \frac{1}{\Delta t} + S_1 + \frac{U_1}{\Delta z}.$$

In view of the iterative character of the suggested method, the computations should satisfy the following condition:

$$\frac{\left|Y_{j,(k+1)}^{t+\Delta t} - Y_{j,(k)}^{t+\Delta t}\right|}{Y_{j,(k+1)}^{t+\Delta t}} \le \vartheta \tag{44}$$

where Y is the currently evaluated temperature in node j; ϑ is the assumed tolerance of iteration; and $k = 1, 2, \ldots$ is the next iteration counter after a single time step.
Additionally, the following condition – the Courant–Friedrichs–Lewy stability condition over the time step – should be satisfied (Gerald, 1994):

$$\left|\beta\right| \le 1, \quad \Delta t \le \frac{\Delta z}{w}, \tag{45}$$

where: $\beta = \dfrac{w\Delta t}{\Delta z}$ is the Courant number.

When satisfying this condition, the numerical solution is reached with a speed $\Delta z/\Delta t$, which is greater than the physical speed w.

3. Computational verification

The efficiency of the proposed method is verified in this section by the comparison of the results obtained using the method and from the corresponding analytical solutions. Exact solutions available in the literature for transient states are developed only for the simplest cases. In this section a step function change of the fluid temperature at the tube inlet and a step function heating on the outer surface of the tube are analysed.

3.1 Analytical solutions for transient states

The available analytical dependencies allow the following to be determined (Serov & Korolkov, 1981):

- the time-spatial temperature distribution of the tube wall, insulated on the outer surface, as the tube's response to the temperature step function of the fluid at the tube inlet,
- the time-spatial temperature distribution of the fluid in the case of a heat flux step function on the outer surface of the tube.

3.1.1 Temperature step function of the fluid at the tube inlet

The analysed step function is assumed as follows (Fig. 4):

$$\Delta T(t) = \begin{cases} 0 & \text{for} \quad t < 0, \\ 1 & \text{for} \quad t \ge 0. \end{cases} \tag{46}$$

For this step function, the dimensionless dependency determining the increase of the tube wall temperature takes the following form:

$$\frac{\Delta\theta}{\Delta T} = V_1 - V_0, \tag{47}$$

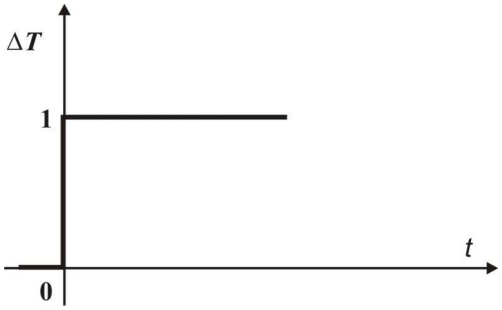

Fig. 4. Temperature step function of the fluid at the tube inlet

where:

$$V_1 = e^{-(\zeta+\eta)} U(\zeta,\eta), \tag{48}$$

$$V_0 = e^{-(\zeta+\eta)} I_0\left(2\sqrt{\zeta\eta}\right). \tag{49}$$

The $U(\zeta,\eta)$ function is described by the following dependency:

$$U(\zeta,\eta) = \sum_{n=0}^{\infty}\sum_{k=0}^{n} \frac{\eta^n \zeta^k}{n!k!}, \tag{50}$$

and the Bessel function:

$$I_0\left(2\sqrt{\zeta\eta}\right) = \sum_{k=0}^{\infty} \frac{(\zeta\eta)^k}{(k!)^2}. \tag{51}$$

Values ζ and η present in Formulae (48)–(51) are the dimensionless variables of length and time respectively, expressed by the following dependencies:

$$\zeta = \frac{z}{F_2}; \qquad \eta = \frac{t - t_{TP}(z)}{D_2}, \tag{52}$$

where:

$$t_{TP}(z) = B_2\zeta = \frac{z}{w}. \tag{53}$$

Coefficients B_2, D_2, and F_2 are described in Section 3.2.

3.1.2 Heat flux step function on the outer surface of the tube

A dimensionless time-spatial function describing the increase of the fluid temperature ΔT, caused by the heat flux step function Δq on the outer surface of the tube, is expressed as:

$$\varphi_1 = \frac{\Delta T}{-\frac{c}{1-c}E_2 \Delta q} = \frac{t}{D_2} - \frac{1}{1-c}\varphi_0 - V_2 \,. \tag{54}$$

In the above formula:
$c = -D_2/B_2$; Δq and coefficient E_2 are described in Section 3.2.
Functions φ_0 and V_2 are described by the following dependencies:

$$\varphi_0 = 1 - e^{-(1-c)\frac{t}{D_2}} - V_1 + V_{00} \,, \tag{55}$$

$$V_2 = e^{-(\zeta+\eta)}\left[(\eta-\zeta)\ U(\zeta,\eta) + \zeta\ I_0\left(2\sqrt{\zeta\eta}\right) + \sqrt{\zeta\eta} I_1\left(2\sqrt{\zeta\eta}\right)\right], \tag{56}$$

where:

$$I_1\left(2\sqrt{\zeta\eta}\right) = \sum_{k=0}^{\infty} \frac{(\zeta\eta)^{\frac{2k+1}{2}}}{(k!)(k+1)!} \,. \tag{57}$$

Function V_{00} present in Formula (55) is expressed as:

$$V_{00} = e^{-(\zeta+\eta)} U\left(\frac{\zeta}{c}, c\eta\right). \tag{58}$$

The analytical dependencies (47) and (54) presented above allow the time-spatial temperature increases, $\Delta\theta$ for the tube wall and ΔT for the fluid, to be determined for any selected cross-section. The results are obtained beginning from time t_{TP} (z) = z/w, that is, from the moment this cross-section is reached by the fluid flowing with velocity w. For example, if the flow velocity equals 1m/s, then the analytical solutions allow the temperature changes for the cross-section located 10 m away from the inlet of the tube to be determined only after 10 s.

3.2 Application of the proposed method for the purpose of verification

In order to compare the results obtained using the suggested method with the results of analytical solutions for transient states, the appropriate dependencies are derived for the control volume shown in Fig. 5.
Assuming one control volume of the tube wall, Equation (4) takes the form of Equation (20). Taking into consideration the boundary conditions:

$$k_w(\theta)\left.\frac{\partial\theta}{\partial r}\right|_{r=r_o} = q \,, \tag{59}$$

and

$$k_w(\theta)\left.\frac{\partial\theta}{\partial r}\right|_{r=r_{in}} = h\left(\theta|_{r=r_{in}} - T\right) = h(\theta - T) \,, \tag{60}$$

the following differential equation is obtained:

$$D_2 \frac{\mathrm{d}\theta}{\mathrm{d}t} = T - \theta + E_2 \Delta q \,. \tag{61}$$

In the above equation:

$$D_2 = \frac{c_w(\theta)\rho_w(\theta)\, d_m\, g_w}{h d_{in}}, \quad E_2 = \frac{1}{h\pi d_{in}}, \text{ and } \quad d_m = \frac{d_o + d_{in}}{2}.$$

Moreover, the heat flux step function is described as:

$$\Delta q = q \cdot s \,, \tag{62}$$

where:
q – heat flux, W/m^2,
s – actual tube pitch, m.

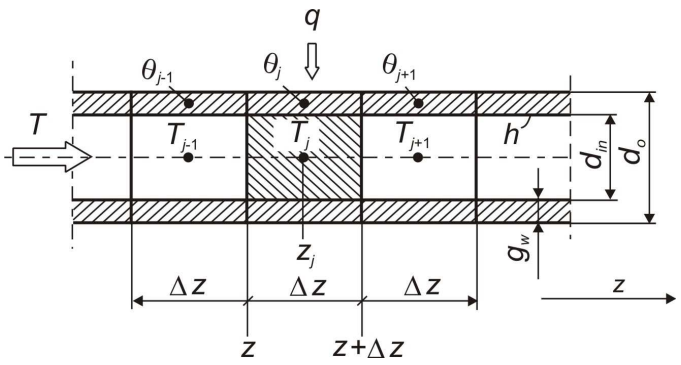

Fig. 5. Analysed control volume

On the side of the working fluid the energy balance equation takes the form of Equation (13), in which the mean wall temperature θ is used instead of θ_h:

$$\Delta z A c(T,p)\rho(T,p)\frac{\Delta T}{\Delta t} = \dot{m}\, i\Big|_z - \dot{m}\, i\Big|_{z+\Delta z} + h\pi d_{in}\Delta z(\theta - T). \tag{63}$$

Assuming that $\Delta t \to 0$ and $\Delta z \to 0$, the following equation is obtained:

$$B_2 \frac{\partial T}{\partial t} = \theta - T - F_2 \frac{\partial T}{\partial z}, \tag{64}$$

where:

$$B_2 = \frac{A c(T,p)\rho(T,p)}{h\pi d_{in}}, \quad F_2 = \frac{\dot{m} c(T,p)}{h\pi d_{in}} \quad \text{and} \quad A = \frac{\pi d_{in}^{\,2}}{4}.$$

To solve the system of Equations (61) and (64), the implicit finite difference method was used, and after transformations we obtain:

$$\theta_j^{t+\Delta t} = \left(\frac{D_2}{D_2 + \Delta t}\right)\theta_j^t + \left(\frac{\Delta t}{\Delta t + D_2}\right)\left(T_j^{t+\Delta t} + E_2 \Delta q_j^{t+\Delta t}\right), \quad j = 1, ..., M \tag{65}$$

$$T_j^{t+\Delta t} = \frac{\theta_j^{t+\Delta t} + \frac{B_2}{\Delta t} T_j^t + \frac{F_2}{\Delta z} T_{j-1}^{t+\Delta t}}{\frac{B_2}{\Delta t} + \frac{F_2}{\Delta z} + 1}, \quad j = 2, ..., M. \tag{66}$$

3.3 Results and discussion

As an illustration of the accuracy and effectiveness of the suggested method the following numerical analyses are carried out:

- for the tube with the temperature step function of the fluid at the tube inlet,
- for the tube with the heat flux step function on the outer surface.

The results obtained are compared afterwards with the results of analytical solutions. In both cases the working fluid is assumed to be water. The heat transfer coefficient is taken as constant and equals $h = 1000$ W/(m²K). Because the exact solutions do not allow the temperature dependent thermo-physical properties to be considered, the following constant water properties were assumed for the computations: $\rho = 988$ kg/m³ and $c = 4199$ J/(kgK). For both cases it was also assumed that the tube is $L = 131$ m long, its external diameter equals $d_o = 0.038$ m, the wall thickness is $g_w = 0.0032$ m, and the tube is made of K10 steel of the following properties: $\rho_w = 7850$ kg/m³ and $c_w = 470$ J/(kgK). Satisfying the Courant condition (45), the following were taken for the computations: $\Delta z = 0.5$ m, $\Delta t = 0.1$ s and $w = 1$ m/s ($\dot{m} = 0.775$ kg/s).

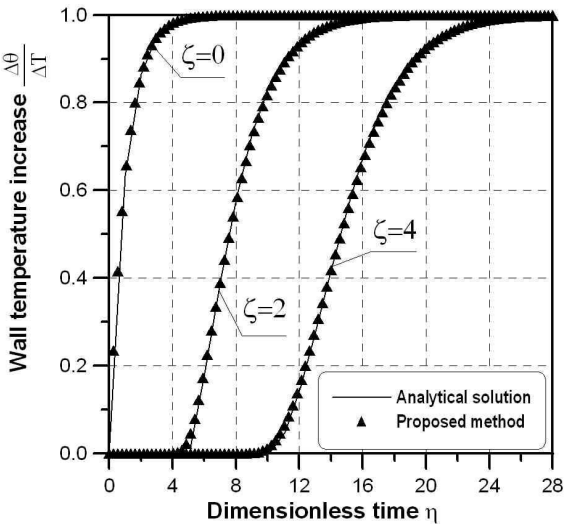

Fig. 6. Dimensionless histories of tube wall temperature increase

In the first numerical analysis it was assumed that water of initial temperature $T = 20$ °C flows through the tube. Also, the tube wall for the initial time $t = 0$ has the same initial temperature. Beginning from the next time step, the fluid of temperature $T = 100$ °C appears at the inlet. The temperature step function is thus $\Delta T = 80$ K. The results of the computations are presented in Fig. 6. The presented dimensionless coordinates $\zeta = 0$, 2, and 4 correspond with the dimensional coordinates $z = 0$, 65.5 m, and 131 m respectively. An analysis of the comparison shows satisfactory convergence of the exact solution results with the results obtained using the presented method.

In the second case it was assumed that the working fluid and the tube at time $t = 0$ take the initial temperature $T = \theta = 70$ °C. Starting from the next time step, the heat flux step function ($\Delta q = q \cdot s$) appears on the outer surface of the tube. The assumed heat load is the heat flux $q = 10^5$ W/m^2 and the tube pitch $s = 0.041$ m. The selected results of the numerical analysis, comprising a comparison of the dimensionless histories of the fluid temperature increase for the same cross-sections as in the first case, are shown in Fig. 7.

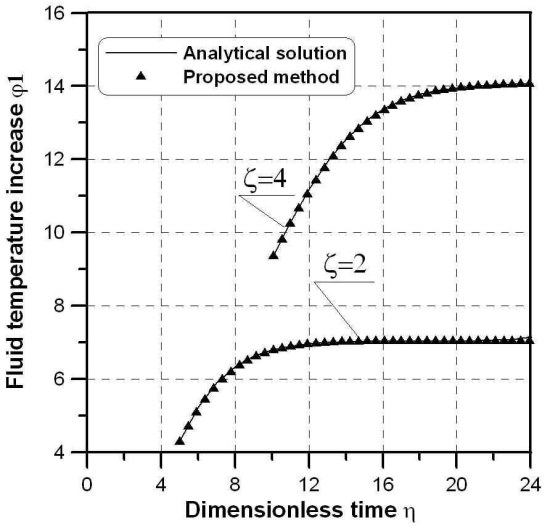

Fig. 7. Histories of dimensionless fluid temperature increase

These histories begin from the time instants $\eta = 5.04$ ($t = 65.5$ s), and $\eta = 10.08$ ($t = 131$ s), respectively, that is, from the moment the analysed cross-sections were reached by the fluid flowing with the velocity $w = 1$ m/s. A satisfactory convergence of the results of the analytical solution with the results obtained using the suggested method was achieved.

4. Experimental verification

This section describes the experimental verification of the proposed method for modelling transient processes which occur in power boilers surfaces heated convectively. Transient state operation of the platen superheater during the start-up of an OP-210 boiler was analysed. The boiler capacity is $210 \cdot 10^3$ kg/h of live steam with 9.8 MPa pressure and 540^{+5}_{-10} °C temperature. The platen superheater (Figs. 8 and 13) consists of 14 vertical screens

installed with 520 mm transversal pitch. Each screen consists of 13 tubes (ϕ 32 × 5 mm) placed with 36 mm longitudinal pitch. The heated surface of the superheater is 406 m² (n = 182 tubes) and the total free cross-section of the combustion gases flow is $A_{cg,t}$ = 64.5 m². The tubes, each L = 26.3 m long, are made of 12H1MF steel and placed in 52 rows. As the analysed platen superheater is operating in cross-parallel-flow, a parallel-flow arrangement was assumed for numerical modelling.

The time-spatial heat transfer coefficients for steam and combustion gases were computed in the on-line mode using dependencies published in (Kuznetsov et al., 1973). Moreover, based on the data given by (Meyer et al., 1993; Kuznetsov et al., 1973; Wegst, 2000) appropriate functions were created. These functions allow the thermo-physical properties of the steam, combustion gases and the material of the tube wall to be computed in real time.

The platen superheater tube was divided into M = 16 cross-sections (Δz = 1.75 m). The time step of computations was taken at Δt = 0.1 s.

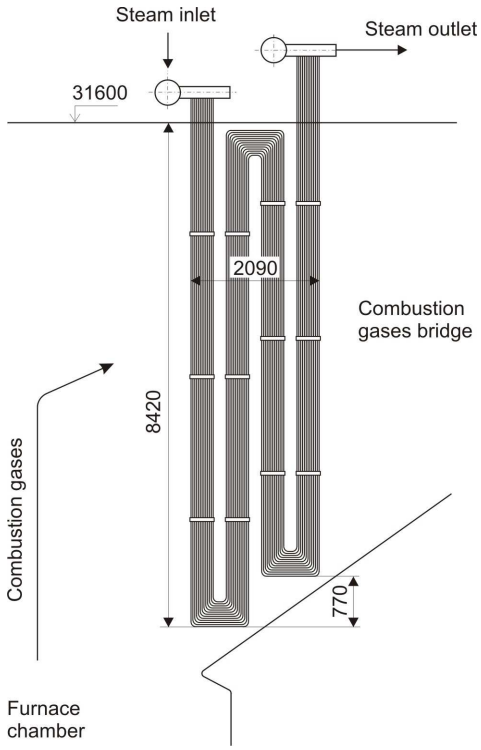

Fig. 8. Location of platen superheater

In order to model the dynamics of the platen superheater it is necessary to know the transient values of temperature, pressure, and total mass flow of steam and combustion gases at the superheater inlet. On the steam side, these values were known from measurements and are shown in Figs. 9 and 11 (curve b), whereas at the combustion gases side they were computed (Fig. 10). To calculate the pressure drop of the steam (in the direction of the steam flow), the Darcy-Weisbach equation was used.

The selection of a platen superheater for verification was not accidental. It is, namely, located in the combustion gas bridge, just behind the furnace chamber (Fig. 8). The computed values of combustion gases temperature and mass flow at the furnace chamber outlet therefore constituted the input data for modelling the platen superheater operation. In order to compute these transient values, the fuel mass flow should be determined first. To find it, a method based on the known characteristics of the coal dust feeder in function of its number of revolutions was used (Cwynar, 1981). The total mass flow of combustion gases at the furnace chamber outlet was computed using stoichiometric combustion equations and the known mass flow of combustion coal. The combustion gases temperature at the furnace chamber outlet was determined by solving the equations of energy and heat transfer for the boiler furnace chamber using the CKTI method (Kuznetsov et al., 1973). The computed values of combustion gases temperature and mass flow are shown in Fig. 10.

The measurements carried out on the real object were disturbed by errors resulting from the degree of inaccuracy of the measuring sensors and converters.

These errors, related to the maximum measuring ranges, were as follows:

a. ± 3.3 °C in the superheated steam temperature readings (measuring range: 0–600 °C; level of sensor inaccuracy: 0.25; level of converter inaccuracy: 0.3),
b. $\pm 96 \cdot 10^3$ Pa in the superheated steam pressure readings (measuring range: 0–16 MPa; level of sensor inaccuracy: 0.6),
c. ± 0.799 kg/s in the mass flow of superheated steam (measuring range: 0–69.44 kg/s; level of measuring orifice inaccuracy: 1; level of converter inaccuracy: 0.15).

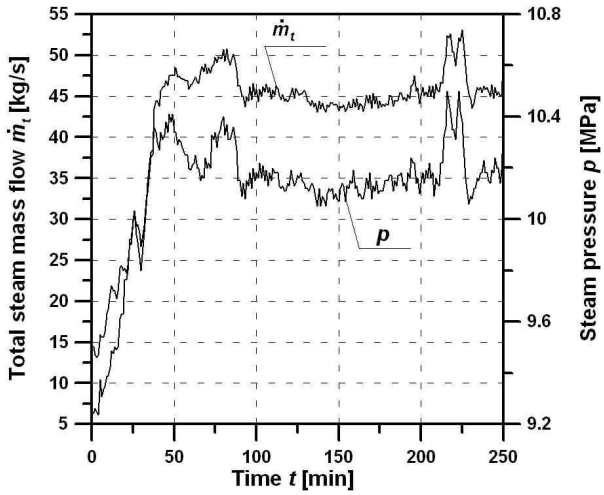

Fig. 9. Histories of the measured steam pressure and total mass flow at the platen superheater inlet

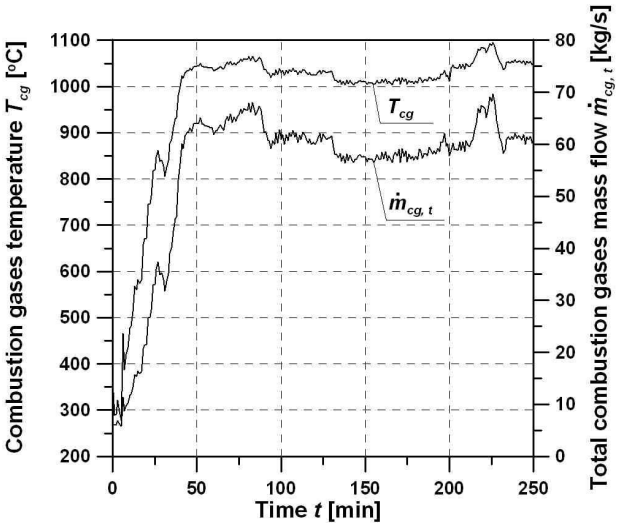

Fig. 10. Histories of the computed combustion gases temperature and total mass flow at the platen superheater inlet (at the furnace chamber outlet)

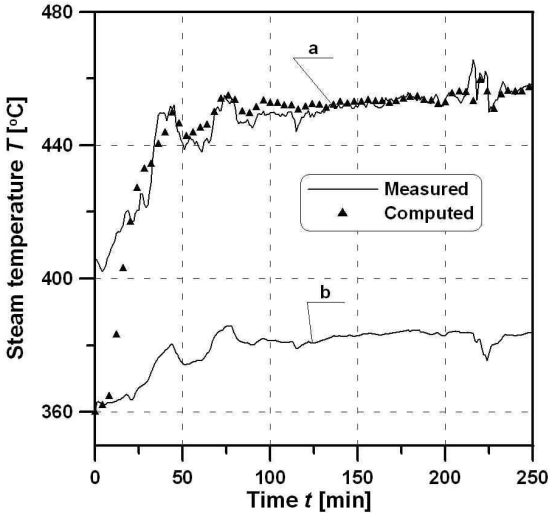

Fig. 11. Comparison of the measured and computed steam temperatures at the superheater outlet (a) and history of the measured steam temperature at the superheater inlet (b)

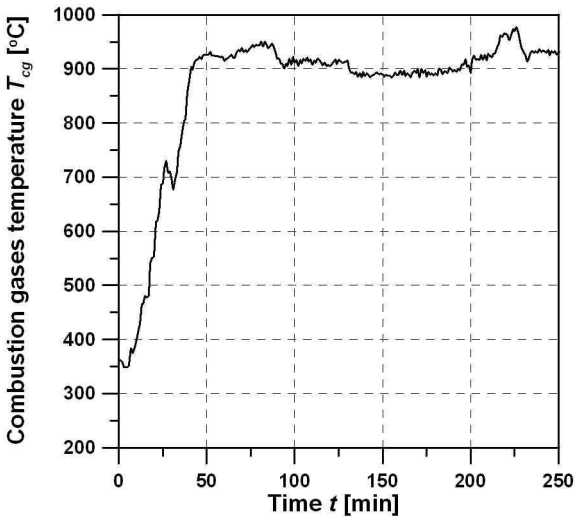

Fig. 12. History of the computed combustion gases temperature at the superheater outlet

When comparing the results of steam temperature measurement at the platen superheater outlet with the results of numerical computation, fully satisfactory convergence is found (Fig. 11 – curve a). The divergences visible in Fig. 11 (curve a), in the range of 0 to about 30 min, result from the assumption in the calculation model that the initial temperature of the analysed steam superheating system at time $t = 0$ is equal to the measured steam temperature at the superheater inlet, that is, $T = T_{cg} = \theta_h = \theta_{cg} = 359$ °C.

The computed combustion gases temperature at the platen superheater outlet (Fig. 12) can be used for modelling the dynamics of steam superheaters located after it (Fig. 13). The two stages, KPP-2 and KPP-3, of the superheater are installed parallel to each other in one gas pass. The superheater KPP-2 operates in counter-flow, and KPP-3 operates in parallel-flow to combustion gases. A comparison of the measured and computed steam temperature histories at the KPP-3 outlet is presented in the paper (Zima, 2003).

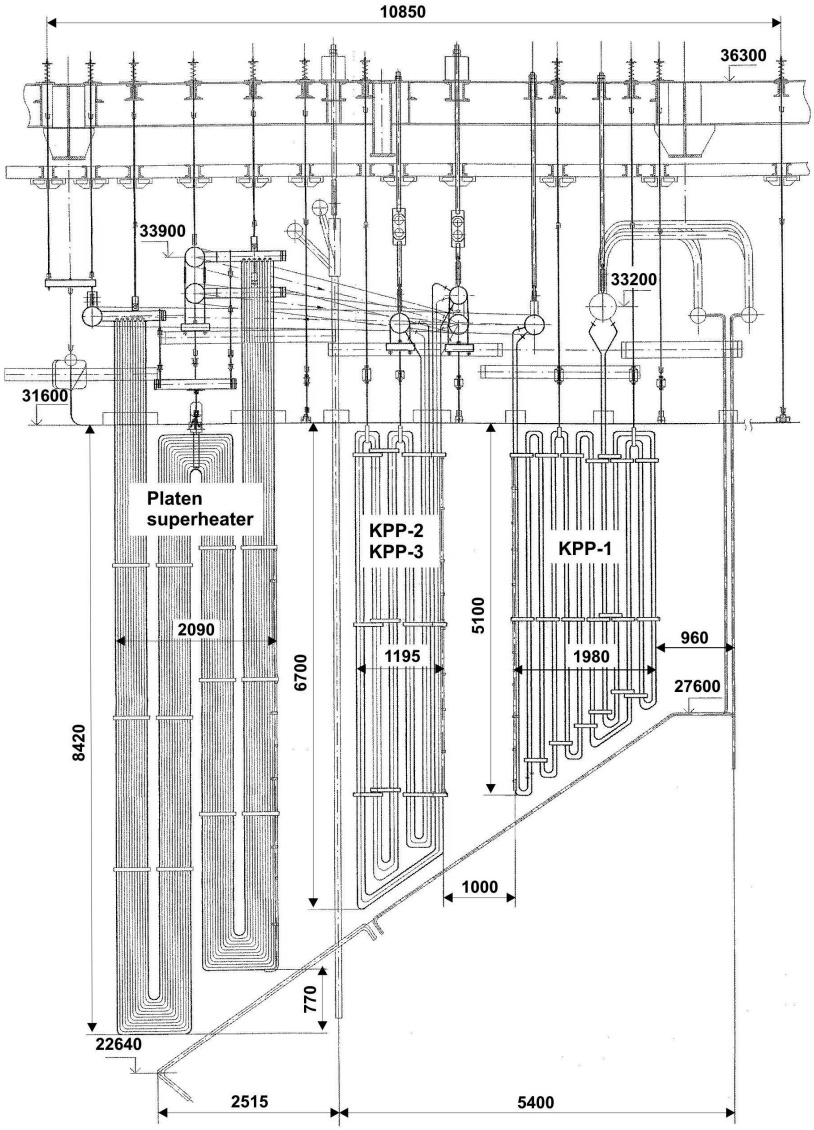

Fig. 13. Location of the analysed platen superheater and three stages of convective steam superheater (KPP-1, KPP-2, and KPP-3)

The selected results of modelling the dynamics of the economizer installed in the convective duct of the OP-210 boiler are presented in the paper (Zima, 2007). In the computations the fins were considered on the combustion gases side, and the heat transfer coefficient was calculated according to (Taler & Duda, 2006). The measured history of feed water temperature at the economizer outlet was compared with the computational results and satisfactory agreement was achieved.

5. Conclusions

The chapter presents a method for modelling the dynamics of boiler surfaces heated convectively, namely steam superheaters and economizers. The proposed method comprises solving the energy equations and considers the superheater or economizer model as one with distributed parameters. The proposed model is one-dimensional and is suitable for pendant superheaters and economizers. In this model, the boundary conditions can be time-dependent. The computations are carried out in the direction of the heated fluid flow in one tube. The time-spatial temperature history of the separating wall is determined from the equation of transient heat conduction. As the time-spatial heat transfer coefficients at the working fluids sides are computed in the on-line mode considering the actual tube pitches and cross-flow of combustion gases, the physics of the phenomena occurring in the superheaters and economizers does not change. All the thermo-physical properties of the fluids and the material of the separating walls are also computed in real time. In order to prove the accuracy and effectiveness of the proposed method, computational and experimental verifications were carried out. The analysis of the presented comparisons demonstrates fully satisfactory convergence of the results obtained using the suggested method with the results of analytical solutions and with measured temperature history. When analysing the presented comparisons it should be considered that many parameters affect the final result of the operation of the surfaces heated convectively (e.g. ones resulting from gradual fouling of these surfaces). Not all these parameters can be fully taken into consideration in the calculation algorithm.

6. References

Bojić, M. & Dragićević, S. (2006). Optimization of steam boiler design. *Proceedings of the Institution of Mechanical Engineers, Part A: Journal of Power and Energy*, Vol. 220, No. 6 (September 2006), pp. 629–634, ISSN 0957-6509

Chakraborty, N. & Chakraborty, S. (2002). A generalized object-oriented computational method for simulation of power and process cycles. *Proceedings of the Institution of Mechanical Engineers, Part A: Journal of Power and Energy*, Vol. 216, No. 2 (April 2002), pp. 155–159, ISSN 0957-6509

Cwynar, L. (1981). *Start-up of Power Boilers* (in Polish), Scientific and Technical Publishing Company, ISBN 83-204-0416-9, Warsaw

Dechamps, P.J. (1995). Modelling the transient behaviour of heat recovery steam generators. *Proceedings of the Institution of Mechanical Engineers, Part A: Journal of Power and Energy*, Vol. 209, No. A4 (January 1995), pp. 265–273, ISSN 0957-6509

Enns, M. (1962). Comparison of dynamic models of a superheater. *ASME Transactions – Journal of Heat Transfer*, Vol. 84, No. 4, pp. 375–385

Gerald, C.F. & Wheatley, P.O. (1994). *Applied numerical analysis*, Addison-Wesley Publishing Company, ISBN 0-201-56553-6, New York

Hausen, H. (1976). *Wärmeübertragung im Gegenstrom, Gleichstrom und Kreuzstrom* (2nd ed.), Springer Verlag, ISBN 3540075526, Berlin

Krzyżanowski, J. & Głuch, J. (2004). *Heat-Flow Diagnostics of Energetic Objects* (in Polish), Polish Academy of Sciences, ISBN 83-88237-65-9, Gdansk

Kuznetsov, N.V.; Mitor, V.V.; Dubovskij, I.E. & Karasina, E.S. (1973). *Standard Methods of Thermal Design for Power Boilers* (in Russian), Central Boiler and Turbine Institute, Energija, UDK 621.181.001.24:536.7, Moscow

Lu, S. (1999). Dynamic modelling and simulation of power plant systems. *Proceedings of the Institution of Mechanical Engineers, Part A: Journal of Power and Energy*, Vol. 213, No. 1 (February 1999), pp. 7–22, ISSN 0957-6509

Meyer, C. A. et al. (1993). *ASME Steam Tables*, American Society of Mechanical Engineers, ISBN 0791806324, New York

Mohammadzaheri, M.; Chen, L.; Ghaffari, A. & Willison, J. (2009). A combination of linear and nonlinear activation functions in neural networks for modeling a de-superheater. *Simulation Modelling Practice & Theory*, Vol. 17, No. 2 (February 2009), pp. 398–407, ISSN 1569190X

Mohan, M.; Gandhi, O.P. & Agrawal, V.P. (2003). Systems modelling of a coal-based steam power plant. *Proceedings of the Institution of Mechanical Engineers, Part A: Journal of Power and Energy*, Vol. 217, No. 3 (June 2003), pp. 259–277, ISSN 0957-6509

Serov, E.P. & Korolkov, B.P. (1981). *Dynamics of Steam Generators* (in Russian), Energoizdat, UDK 621.181.016.7, Moscow

Shirakawa, M. (2006). Development of a thermal power plant simulation tool based on object orientation. *Proceedings of the Institution of Mechanical Engineers, Part A: Journal of Power and Energy*, Vol. 220, No. 6 (September 2006), pp. 569–579, ISSN 0957-6509

Taler, J. & Duda, P. (2006). *Solving Direct and Inverse Heat Conduction Problems*, Springer, ISBN 978-3-540-33470-5, Berlin

Wegst, C.W. (2000). *Key to Steel*, Verlag Stahlschlüssel Wegst GmbH, ISBN 3922599176, Marbach

Zima, W. (2001). Numerical modeling of dynamics of steam superheaters. *Energy*, Vol. 26, No. 12, (December 2001), pp. 1175–1184, ISSN 0360-5442

Zima, W. (2003). Mathematical model of transient processes in steam superheaters. *Forschung im Ingenieurwesen*, Vol. 68, No. 1 (July 2003), pp. 51–59, ISSN 0015-7899

Zima, W. (2004). *Simulation of transient processes in boiler steam superheaters* (in Polish), Monograph 311, Publishing House of Cracow University of Technology, ISSN 0860-097X, Cracow

Zima, W. (2006). Simulation of dynamics of a boiler steam superheater with an attemperator. *Proceedings of the Institution of Mechanical Engineers, Part A: Journal of Power and Energy*, Vol. 220, No. 7 (November 2006), pp. 793–801, ISSN 0957-6509

Zima, W. (2007). Mathematical modelling of transient processes in convective heated surfaces of boilers. *Forschung im Ingenieurwesen*, Vol. 71, No. 2 (June 2007), pp. 113–123, ISSN 0015-7899

Heat Transfer - Engineering Applications

Edited by Prof. Vyacheslav Vikhrenko

ISBN 978-953-307-361-3
Hard cover, 400 pages
Publisher InTech
Published online 22, December, 2011
Published in print edition December, 2011

Heat transfer is involved in numerous industrial technologies. This interdisciplinary book comprises 16 chapters dealing with combined action of heat transfer and concomitant processes. Five chapters of its first section discuss heat effects due to laser, ion and plasma-solid interaction. In eight chapters of the second section engineering applications of heat conduction equations to the curing reaction kinetics in manufacturing process, their combination with mass transport or ohmic and dielectric losses, heat conduction in metallic porous media and power cables are considered. Analysis of the safety of mine hoist under influence of heat produced by mechanical friction, heat transfer in boilers and internal combustion engine chambers, management for ultrahigh strength steel manufacturing are described in this section as well. Three chapters of the last third section are devoted to air cooling of electronic devices.

How to reference

In order to correctly reference this scholarly work, feel free to copy and paste the following:

Wiesław Zima (2011). Mathematical Modelling of Dynamics of Boiler Surfaces Heated Convectively, Heat Transfer - Engineering Applications, Prof. Vyacheslav Vikhrenko (Ed.), ISBN: 978-953-307-361-3, InTech, Available from: http://www.intechopen.com/books/heat-transfer-engineering-applications/mathematical-modelling-of-dynamics-of-boiler-surfaces-heated-convectively

INTECH
open science | open minds

InTech Europe
University Campus STeP Ri
Slavka Krautzeka 83/A
51000 Rijeka, Croatia
Phone: +385 (51) 770 447
Fax: +385 (51) 686 166
www.intechopen.com

InTech China
Unit 405, Office Block, Hotel Equatorial Shanghai
No.65, Yan An Road (West), Shanghai, 200040, China
中国上海市延安西路65号上海国际贵都大饭店办公楼405单元
Phone: +86-21-62489820
Fax: +86-21-62489821

© 2011 The Author(s). Licensee IntechOpen. This is an open access article distributed under the terms of the Creative Commons Attribution 3.0 License, which permits unrestricted use, distribution, and reproduction in any medium, provided the original work is properly cited.